Synthesis and Characterization of Hexagonally Ordered Carbon Nanopipes

Michal Kruk,[†] Mietek Jaroniec,*[,†] Tae-Wan Kim,[‡] and Ryong Ryoo*[,‡]

Department of Chemistry, Kent State University, Kent, Ohio 44242, and National Creative Research Initiative Center for Functional Nanomaterials, and Department of Chemistry (School of Molecular Science-BK21), Korea Advanced Institute of Science and Technology, Daejeon, 305-701, Korea

Received February 21, 2003. Revised Manuscript Received May 5, 2003

CMK-5 ordered mesoporous carbons that consist of two-dimensional (2-D) hexagonal arrays of pipes were synthesized using furfuryl alcohol as a carbon source and SBA-15 aluminosilicate of 2-D hexagonal structure as a template. External and internal pipe diameters were varied concomitantly by using SBA-15 templates with different pore diameters. The internal pipe diameter was also adjustable by changing conditions of the deposition of the carbon film on the walls of the template. It was shown that, under the typical synthesis conditions, furfuryl alcohol is fully polymerized inside SBA-15 pores. The internal pores of the pipes are generated during pyrolysis of the furfuryl alcohol under vacuum conditions. These pores are quite uniform in diameter, although there was evidence for the presence of constrictions in them, which may be related to the internal surface roughness or corrugation. The thickness of the carbon layer on the walls of the SBA-15 template was estimated as a difference between the pore radius of the template and the pore radius of the SBA-15/carbon composite, and it was found to be in the range 0.6−1.3 nm. This value is expected to correspond to the thickness of the walls of the carbon tubes, although the walls may be locally much thicker because of the occurrence of roughness or corrugation of the internal surface of the tubes. Despite the fact that the SBA-15/carbon composites exhibited moderate specific surface areas and pore volumes, the CMK-5 carbons obtained after the SBA-15 template removal exhibited very high nitrogen BET specific surface areas (about 2000 $m^2 g^{-1}$) and total pore volumes (about 1.5 $cm^3 g^{-1}$), which is likely to be related to a unique surface-templated structure of CMK-5 carbons. The internal volume of the mesoporous pipes tended to be smaller than the volume of mesopores between the pipes.

1. Introduction

The past five years have brought major developments in the templated synthesis of porous carbons,[1−7] which includes the successful synthesis of carbons with ordered macropores (width above 50 nm), mesopores (width between 2 and 50 nm), and micropores (width below 2 nm). In 1998, the synthesis of ordered macroporous carbons using colloidal crystals as templates was reported,[8] and this promising direction of research was further pursued later.[9−12] In 1999, the successful synthesis of ordered mesoporous carbons (OMCs) was disclosed.[13,14] In this case, ordered mesoporous silicas (OMSs) were employed as templates. In 2000, the pursuit for an ordered microporous carbon[5−7] was successfully finalized through a two-step carbon infiltration of the zeolite template.[15,16] The synthesis of OMCs was found to be particularly robust from the point of view of obtaining different types of ordered structures, owing to the diversity in the achievable 3-dimensional (3-D) structures of the OMS templates. In particular, CMK-1 carbon[13,14,17−32] with $I4_1/a$ (or lower) symmetry[24,25] and

* Correspondence should be addressed to Prof. M. Jaroniec (phone, 330-672-3790; fax, 330-672-3816; e-mail, jaroniec@kent.edu) and Prof. R. Ryoo (e-mail, rryoo@webmail.kaist.ac.kr).

[†] Kent State University.

[‡] Korea Advanced Institute of Science and Technology.

(1) Knox, J. H.; Kaur, B.; Millward, G. R. *J. Chromatogr.* **1986**, *352*, 3.

(2) Bandosz, T. J.; Jagiello, J.; Putyera, K.; Schwarz, J. A. *Chem. Mater.* **1996**, *8*, 2023.

(3) Kyotani, T.; Tsai, L.-f.; Tomita, A. *Chem. Mater.* **1996**, *8*, 2109.

(4) Che, G.; Lakshimi, B. B.; Martin, C. R.; Fisher, E. R.; Ruoff, R. S. *Chem. Mater.* **1998**, *10*, 260.

(5) Kyotani, T.; Nagai, T.; Inoue, S.; Tomita, A. *Chem. Mater.* **1997**, *9*, 609.

(6) Johnson, S. A.; Brigham, E. S.; Ollivier, P. J.; Mallouk, T. E. *Chem. Mater.* **1997**, *9*, 2448.

(7) Rodriguez-Mirasol, J.; Cordero, T.; Radovic, L. R.; Rodriguez, J. J. *Chem. Mater.* **1998**, *10*, 550.

(8) Zakhidov, A. A.; Baughman, R. H.; Iqbal, Z.; Cui, C.; Khayrullin, I.; Dantas, S. O.; Marti, J.; Ralchenko, V. G. *Science* **1998**, *282*, 897.

(9) Lei, Z.; Zhang, Y.; Wang, H.; Ke, Y.; Li, J.; Li, F.; Xing, J. *J. Mater. Chem.* **2001**, *11*, 1975.

(10) Yu, J.-S.; Yoon, S. B.; Chai, G. S. *Carbon* **2001**, *39*, 1421.

(11) Kang, S.; Yu, J.-S.; Kruk, M.; Jaroniec, M. *Chem. Commun.* **2002**, 1670.

(12) Yu, J.-S.; Kang, S.; Yoon, B.; Chai, G. *J. Am. Chem. Soc.* **2002**, *124*, 9382.

(13) Ryoo, R.; Joo, S. H.; Jun, S. *J. Phys. Chem. B* **1999**, *103*, 7743.

(14) Lee, J.; Yoon, S.; Hyeon, T.; Oh, S. M.; Kim, K. B. *Chem. Commun.* **1999**, 2177.

(15) Ma, Z.; Kyotani, T.; Tomita, A. *Chem. Commun.* **2000**, 2365.

(16) Ma, Z.; Kyotani, T.; Tomita, A. *Carbon* **2002**, *40*, 2367.

(17) Yoon, S.; Lee, J. W.; Hyeon, T.; Oh, S. M. *J. Electrochem. Soc.* **2000**, *147*, 2507.

(18) Kruk, M.; Jaroniec, M.; Ryoo, R.; Joo, S. H. *J. Phys. Chem. B* **2000**, *104*, 7960.

(19) Yoon, S. B.; Kim, J. Y.; Yu, J.-S. *Chem. Commun.* **2001**, 559.

10.1021/cm034087+ CCC: $25.00
Published on Web 06/03/2003

CMK-4 carbon with cubic *Ia*3*d* symmetry[24,33] were synthesized using MCM-48[34,35] and FDU-5[36,37] silica templates of *Ia*3*d* symmetry. CMK-2 carbon[22,32] with cubic *Pm*3*n* symmetry was obtained using an SBA-1 template (*Pm*3*n* space group).[38] CMK-3[32,39−48] and CMK-5[49,50] carbons with 2-D hexagonal (*p*6*mm*) symmetry were synthesized using an SBA-15 template (*p*6*mm* symmetry).[51−53] Moreover, the possibility of the synthesis of OMC with cubic *Im*3*m* symmetry using for instance the SBA-16 silica[51] template was discussed during a recent international conference meeting.[54] There are also several other mesoporous carbons related to OMCs, including carbon of disordered structure with uniform mesopores[55] synthesized using HMS silica template,[56] mesoporous carbon foams[57,58] synthesized using silica mesocellular foam template,[59] and carbon with spherical particles featuring mesoporous shells and void cores[60,61] synthesized using hard core−porous shell silica particles.[62]

The discovery of OMCs was a major achievement in the field of synthesis of porous carbons. OMCs and related carbons have already been shown to be promising as electrochemical double-layer capacitors,[14,17,33,55] catalyst supports,[49] and templates for ordered mesoporous inorganic materials.[45,46] Carbon-infiltrated OMSs, which are intermediates in the OMC synthesis, were found suitable as precursors in the synthesis of disordered silicon carbide with quite large specific surface area.[30]

Templated synthesis of ordered carbons potentially offers an additional flexibility of making volume-templated and surface-templated carbons.[8,12,49,50] In the first case, the entire void space of the template is infiltrated with carbon, whereas in the second case, carbon is introduced as a film on the surface of the template. Although first ordered macroporous carbons included both volume-templated and surface-templated materials,[8] initially reported OMCs[13,14,22,32,39] were exclusively volume-templated. Moreover, surface-templated ordered microporous carbon has not been reported. Apparently, the difficulty in the formation of a carbon film on the surface of a silica template increases as the pore diameter of the template decreases, perhaps because it is more difficult to suppress the formation of carbon in the entire volume of the template in cases where the pores of the template are relatively narrow. CMK-5 carbon,[49] which consists of 2-D hexagonally ordered carbon pipes (see Scheme 1), is the only surface-templated OMC reported so far. CMK-5 was synthesized using furfuryl alcohol as a carbon precursor and SBA-15 aluminosilicate as a template.[49] Surface templating was achieved through the control of the amount of the carbon precursor and other synthesis conditions. Alternatively, CMK-5 can be synthesized using a cobalt-containing SBA-15 template through catalytic chemical vapor deposition (CCVD) carried out for appropriately short periods of time using ethylene as a carbon precursor.[50]

The pore size control is an important issue in the OMC synthesis. In the case of some important OMCs,

(20) Joo, S. H.; Jun, S.; Ryoo, R. *Microporous Mesoporous Mater.* **2001**, *44*−*45*, 153.
(21) Ahn, W. S.; Min, K. I.; Chung, Y. M.; Rhee, H.-K.; Joo, S. H.; Ryoo, R. *Stud. Surf. Sci. Catal.* **2001**, *135*, 313.
(22) Ryoo, R.; Joo, S. H.; Jun, S.; Tsubakiyama, T.; Terasaki, O. *Stud. Surf. Sci. Catal.* [CD-ROM] **2001**, *135*.
(23) Darmstadt, H.; Roy, C.; Kaliaguine, S.; Choi, S. J.; Ryoo, R. *Abstracts of Papers* [CD-ROM], Carbon 2001, International Carbon Conference, American Carbon Society: Lexington, KY, July 14−19, 2001.
(24) Kaneda, M.; Tsubakiyama, T.; Carlsson, A.; Sakamoto, Y.; Ohsuna, T.; Terasaki, O.; Joo, S. H.; Ryoo, R. *J. Phys. Chem. B* **2002**, *106*, 1256.
(25) Solovyov, L. A.; Zaikovskii, V. I.; Shmakov, A. N.; Belousov, O. V.; Ryoo, R. *J. Phys. Chem. B* **2002**, *106*, 12198.
(26) Yoon, S. B.; Kim, J. Y.; Yu, J.-S. *Chem. Commun.* **2002**, 1536.
(27) Darmstadt, H.; Roy, C.; Kaliaguine, S.; Choi, S. J.; Ryoo, R. *Carbon* **2002**, *40*, 2673.
(28) Ohkubo, T.; Miyawaki, J.; Kaneko, K.; Ryoo, R.; Seaton, N. A. *J. Phys. Chem. B* **2002**, *106*, 6523.
(29) Vix-Guterl, C.; Boulard, S.; Parmentier, J.; Werckmann, J.; Patarin, J. *Chem. Lett.* **2002**, 1062.
(30) Parmentier, J.; Patarin, J.; Dentzer, J.; Vix-Guterl, C. *Ceram. Int.* **2002**, *28*, 1.
(31) Jun, S.; Choi, M.; Ryu, S.; Lee, H.-Y.; Ryoo, R. *Abstracts of Papers*, 3rd International Mesostructured Materials Symposium, July 8−11, 2002; Korean Zeolite Association: Jeju, Korea, 2002; PA-2, p 52.
(32) Ryoo, R.; Joo, S. H.; Kruk, M.; Jaroniec, M. *Adv. Mater.* **2001**, *13*, 677.
(33) Yang, H.; Shi, Q.; Liu, X.; Xie, S.; Jiang, D.; Zhang, F.; Yu, C.; Tu, B.; Zhao, D. *Chem. Commun.* **2002**, 2842.
(34) Beck, J. S.; Vartuli, J. C.; Roth, W. J.; Leonowicz, M. E.; Kresge, C. T.; Schmitt, K. D.; Chu, C. T−W.; Olson, D. H.; Sheppard, E. W.; McCullen, S. B.; Higgins, J. B.; Schlenker, J. L. *J. Am. Chem. Soc.* **1992**, *114*, 10834.
(35) Monnier, A.; Schuth, F.; Huo, Q.; Kumar, D.; Margolese, D.; Maxwell, R. S.; Stucky, G. D.; Krishnamurty, M.; Petroff, P.; Firouzi, A.; Janicke, M.; Chmelka, B. F. *Science* **1993**, *261*, 1299.
(36) Liu, X.; Tian, B.; Yu, C.; Gao, F.; Xie, S.; Tu, B.; Che, R.; Peng, L.-M.; Zhao, D. *Angew. Chem., Int. Ed.* **2002**, *41*, 3876.
(37) Chan, Y.-T.; Lin, H.-P.; Mou, C.-Y.; Liu, S.-T. *Chem. Commun.* **2002**, 2878.
(38) Huo, Q.; Margolese, D. I.; Ciesla, U.; Feng, P.; Gier, T. E.; Sieger, P.; Leon, R.; Petroff, P. M.; Schuth, F.; Stucky, G. D. *Nature* **1994**, *368*, 317.
(39) Jun, S.; Joo, S. H.; Ryoo, R.; Kruk, M.; Jaroniec, M.; Liu, Z.; Ohsuna, T.; Terasaki, O. *J. Am. Chem. Soc.* **2000**, *122*, 10712.
(40) Shin, H. J.; Ryoo, R.; Kruk, M.; Jaroniec, M., *Chem. Commun.* **2001**, 349.
(41) Kim, S.-S.; Pinnavaia, T. J. *Chem. Commun.* **2001**, 2418.
(42) Joo, S. H.; Ryoo, R.; Kruk, M.; Jaroniec, M. *J. Phys. Chem. B* **2002**, *106*, 4640.
(43) Lee, J.-S.; Joo, S. H.; Ryoo, R. *J. Am. Chem. Soc.* **2002**, *124*, 1156.
(44) Solovyov, L. A.; Shmakov, A. N.; Zaikovskii, V. I.; Joo, S. H.; Ryoo, R. *Carbon* **2002**, *40*, 2477.
(45) Kang, M.; Yi, S. H.; Lee, H. I.; Yie, J. E.; Kim, J. M. *Chem. Commun.* **2002**, 1944.
(46) Lu, A.-H.; Schmidt, W.; Taguchi, A.; Spliethoff, B.; Tesche, B.; Schuth, F. *Angew. Chem., Int. Ed.* **2002**, *41*, 3489.
(47) Yu, C.; Fan, J.; Tian, B.; Zhao, D.; Stucky, G. D. *Adv. Mater.* **2002**, *14*, 1742.
(48) Kruk, M.; Jaroniec, M.; Joo, S. H.; Ryoo, R. *J. Phys. Chem. B* **2003**, *107*, 2205.
(49) Joo, S. H.; Choi, S. J.; Oh, I.; Kwak, J.; Liu, Z.; Terasaki, O.; Ryoo, R. *Nature* **2001**, *412*, 169.
(50) Zhang, W.-H.; Liang, C.; Sun, H.; Shen, Z.; Guan, Y.; Ying, P.; Li, C. *Adv. Mater.* **2002**, *14*, 1776.
(51) Zhao, D.; Huo, Q.; Feng, J.; Chmelka, B. F.; Stucky, G. D. *J. Am. Chem. Soc.* **1998**, *120*, 6024.
(52) Ryoo, R.; Ko, C. H.; Kruk, M.; Antochshuk, V.; Jaroniec, M. *J. Phys. Chem. B* **2000**, *104*, 11465.
(53) Kruk, M.; Jaroniec, M.; Ko, C. H.; Ryoo, R. *Chem. Mater.* **2000**, *12*, 1961.
(54) Yu, C.; Stucky, G. D.; Zhao, D. *Abstracts of Papers*, 3rd International Mesostructured Materials Symposium, July 8−11, 2002; Korean Zeolite Association: Jeju, Korea, 2002; PA-4, p 54.
(55) Lee, J.; Yoon, S.; Oh, S. M.; Shin, C.-H.; Hyeon, T. *Adv. Mater.* **2000**, *12*, 359.
(56) Tanev, P. T.; Pinnavaia, T. J. *Science* **1995**, *267*, 865.
(57) Lee, J.; Sohn, K.; Hyeon, T. *J. Am. Chem. Soc.* **2001**, *123*, 5146.
(58) Lee, J.; Sohn, K.; Hyeon, T. *Chem. Commun.* **2002**, 2674.
(59) Schmidt-Winkel, P.; Lukens, W. W., Jr.; Zhao, D.; Yang, P.; Chmelka, B. F.; Stucky, G. D. *J. Am. Chem. Soc.* **1999**, *121*, 254.
(60) Yoon, S. B.; Sohn, K.; Kim, J. Y.; Shin, C.-H.; Yu, J.-S.; Hyeon, T. *Adv. Mater.* **2002**, *14*, 19.
(61) Kim, M.; Sohn, K.; Na, H. B.; Hyeon, T. *Nano Lett.* **2002**, *2*, 1383.
(62) Buchel, G.; Unger, K. K.; Matsumoto, A.; Tsutsumi, K. *Adv. Mater.* **1998**, *10*, 1036.

Scheme 1. Schematic Illustration of the Structure of CMK-5 Carbon

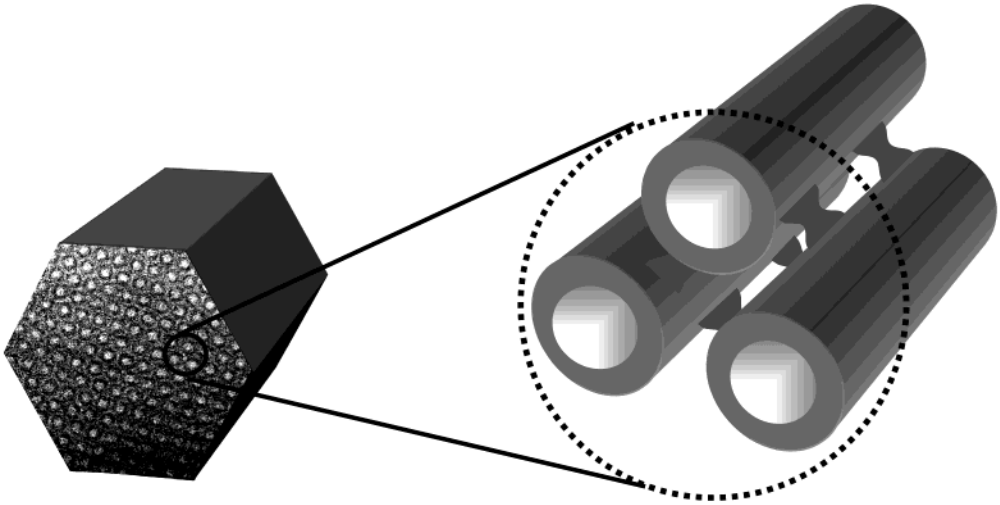

such as CMK-1 and CMK-3, it is quite difficult to obtain samples with appreciably different mesopore diameter,[18,48] largely because of the fact that the pore wall thickness of MCM-48 and SBA-15 templates suitable for the OMC synthesis is not particularly easy to tailor. Recently, this problem was overcome using 2-D hexagonal silica templates synthesized in the presence of mixed cationic−nonionic surfactant assemblies, which allowed one to control the thickness of the walls of the silica templates and, consequently, the pore size of the resultant CMK-3 carbon replicas.[43] The pore size of CMK-3 can also be enlarged by thermally treating the carbon at high temperature under inert atmosphere.[23] It was mentioned in the disclosure of the synthesis of CMK-5 carbon that the internal pipe diameter can be controlled in several ways, including the selection of appropriate conditions of the introduction of the carbon film.[49] Later, the tailoring of the internal pipe diameter was also achieved through the control of the time of the CCVD process.[50]

Herein, the synthesis of CMK-5 carbons with various outer and inner diameters of the pipes using aluminosilicate SBA-15 templates and furfuryl alcohol as a carbon precursor is described in detail. The outer and inner diameters were adjusted concurrently by using an SBA-15 template with a required pore diameter, whereas the inner diameter was adjusted independently by controlling the conditions of the introduction of the carbon film. The thickness of the walls of the carbon pipes was estimated. Moreover, the existence of constrictions inside the carbon pipes was demonstrated using argon adsorption at 77 K, which suggests an appreciable roughness or corrugation of the internal surface of the carbon pipes.

2. Materials and Methods

2.1. Materials. Four samples of the SBA-15-type 2-D hexagonal silica with various pore diameters were synthesized using surfactants of different size or surfactant mixtures. These samples are denoted as samples A−D. The details of the synthesis procedures are as follows: Sample A was synthesized using tetraethyl orthosilicate (TEOS) and the $EO_{20}PO_{70}EO_{20}$ triblock copolymer (Pluronic P123 from BASF), following the SBA-15 synthesis procedure reported previously.[39,51] P123 (4.0 g) was dissolved in 150 g of 1.6 M HCl solution at 308 K. TEOS (8.50 g) was added while the solution was stirred. The stirring was continued for 15 min at the same temperature. This mixture was placed under static conditions in an oven at 308 K for 24 h and subsequently at 373 K for 24 h. Sample B was synthesized in the same way as for sample A, except for the use of sodium silicate solution (1.3 wt % Na_2O, 5.0 wt % SiO_2, and 93.7 wt % H_2O) and the $EO_{17}PO_{60}EO_{17}$ surfactant (Pluronic P103, BASF). That is, 49.6 g of the sodium silicate solution was added to the solution of 4 g of P103 dissolved in 104.2 g of 1.6 M HCl at 308 K. The remainder of the synthesis procedure is the same as for sample A. The synthesis of sample C was carried out with a surfactant mixture consisting of 2.8 g of P103, 0.6 g of the $C_{12}EO_7$ surfactant [$C_{12}H_{25}O(C_2H_5O)_7H$, Hannong LE-7], and 0.6 g $C_{12}EO_5$ (Hannong LE-5), which were dissolved in 105.2 g of 0.86 M HCl solution. To this solution was added 44.8 g of sodium silicate solution at 308 K with stirring. Stirring was continued for 12 h at the same temperature. Then, the resultant mixture was aged at 373 K for 12 h under static conditions. In the case of sample D, the surfactant mixture consisted of 2 g of P103, 1 g of LE-7, and 1 g LE-5. This mixture was dissolved in 103.6 g of 0.86 M HCl solution at 308 K, and then 25.6 g of sodium silicate was added. The remainder of the synthesis procedure was the same as for sample C.

All silica products were filtered without washing, dried at 373 K, washed with ethanol, and calcined at 673 K. The calcined silica samples were impregnated an with aqueous solution of $AlCl_3$ (typically, Si/Al = 20).[63,64] After the solvent water was completely evaporated in a rotary evaporator, the samples were calcined in air at 823 K. The Al incorporation was carried out in order to make the pore wall surface catalytically active in the acid-catalyzed polymerization of furfuryl alcohol.

Four kinds of CMK-5-X samples (X = A, B, C and D) were prepared following the same procedures. The pores of silica templates A, B, C, and D were filled with furfuryl alcohol by incipient wetness infiltration at room temperature. The furfuryl alcohol/SBA-15 composite was heated overnight at 368 K, in a closed bottle for polymerization. The polymerized alcohol was converted to carbon while heated to 1173 K under vacuum. The carbon/silica composites thus obtained were denoted composites A, B, C, and D. Finally, the template walls were removed with HF solution. The resultant carbon samples were denoted CMK-5-A, -B, -C, and -D.

The synthesis procedure for CMK-5-E sample was the same as for CMK-5-A until the pyrolysis temperature was increased to 623 K. The sample was cooled to room temperature after it was heated for 2 h under the vacuum pyrolysis conditions. Then, an additional amount of furfuryl alcohol corresponding

(63) Jun, S.; Ryoo, R. *J. Catal.* **2000**, *195*, 237.
(64) Ryoo, R.; Jun, S.; Kim, J. M.; Kim, M. J. *Chem. Commun.* **1997**, 2225.

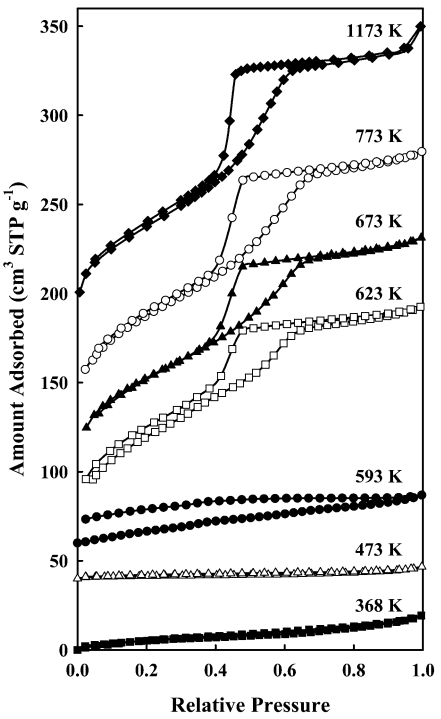

Figure 1. Nitrogen adsorption isotherms for SBA-15 aluminosilicate infiltrated with furfuryl alcohol and subjected to pyrolysis under vacuum at different temperatures. The isotherms corresponding to pyrolysis temperatures of 473, 593, 773, and 1173 K are offset vertically by 40, 60, 40, and 110 cm^3 STP g^{-1}, respectively.

to18% of the total mesopore volume was added to the sample. The sample was heated again at 368 K for polymerization of the furfuryl alcohol. The carbonization of the carbon source was performed with heating to 1173 K under vacuum. The resultant carbon/silica composite and carbon sample were denoted composite E and CMK-5-E, respectively.

2.2. Methods. X-ray diffraction (XRD) patterns of samples were recorded on a Rigaku MultiFlex instrument (operated at 2 kW) using Cu Kα radiation. Nitrogen and argon adsorption isotherms were measured at 77 K on a Micromeritics ASAP 2010 volumetric adsorption analyzer. In the case of argon, the saturation vapor pressure corresponding to gas−solid equilibrium (which was measured during the adsorption run) was used to calculate the relative pressure.[65] Before the adsorption measurements, samples were outgassed at 473 K in the port of the adsorption analyzer. Some nitrogen adsorption isotherms at 77 K (those shown in Figure 1) were also measured on a Quantachrome NOVA 2000 instrument. Weight change curves were recorded under air on a TA Instruments TGA 2950 high-resolution thermogravimetric analyzer in a high-resolution mode. The maximum heating rate was 20 K min^{-1}. For transmission electron microscopy (TEM) imaging, the samples were suspended in ethanol (99.9 vol %) by ultrasonication. The suspension was deposited on a carbon microgrid, and the imaging was performed at room temperature using a 400 kV electron microscope (JEM-4000EX).

2.3. Calculations. The BET specific surface area[66] was calculated from nitrogen adsorption data in the relative pressure range from 0.04 to 0.2. The total pore volume[66] was estimated from the amount of nitrogen adsorbed at a relative pressure of about 0.99. The external surface area and the sum of the primary mesopore volume and the micropore volume were estimated from nitrogen adsorption data using the α_s plot method[66,67] in the α_s range from 1.7 to 2.2 (except for composite D, for which the range 1.3−2.2 was used). It should be noted that α_s is defined as the amount adsorbed at a particular pressure divided by the amount adsorbed at a relative pressure of 0.4.[66,67] The reference adsorption isotherm used in the α_s plot calculations was reported elsewhere.[67] The pore size distributions (PSDs) were calculated from nitrogen and argon adsorption isotherms using a method calibrated for MCM-41 silicas.[65,68] The position of the maximum on the PSD is referred to as the pore diameter.

3. Results and Discussion

3.1. Carbonization of Furfuryl Alcohol in SBA-15 Template. Through carbonization experiments under various conditions, we found out that the most important points in the CMK-5 synthesis using furfuryl alcohol were (i) incorporation of polymerization catalysts onto the template pore walls and (ii) pyrolysis under vacuum conditions. Our results indicated that furfuryl alcohol should be fully cross-linked via the catalytic polymerization and subsequently converted to carbon under vacuum pyrolysis conditions (see section 2.1). The most effective catalysts for the polymerization of furfuryl alcohol were Al and Sn, which could be easily incorporated following the postsynthesis procedure.[63,64] Vacuum pyrolysis after the polymerization led to the formation of the tube-type CMK-5 carbon. Pyrolysis without vacuum or rapid N_2 flow resulted in the formation of the rod-type CMK-3 carbon. However, neither of the ordered mesoporous carbons could be obtained when the silica template was used without catalysts, due to the loss of carbon source during pyrolysis.

The polymerization of furfuryl alcohol resulted in complete filling of the entire pore volume of the SBA-15 template. The nitrogen adsorption isotherms of the polymer/silica composite indicated no significant accessible pore volume until the pyrolysis temperature was increased to 593 K (Figure 1). The adsorption isotherms indicated that mesopores began to develop around 623 K. There was a sudden increase in the XRD intensity at this temperature, in agreement with the pore generation.

3.2. SBA-15/Carbon Composites. XRD patterns for the composites (Figure 2) were similar to the XRD patterns typically reported for SBA-15 silicas[39,51] and characteristic of 2-D hexagonally ordered structure. The unit-cell size gradually decreased for composites from A to D (see Table 1). Composites A and E had similar unit-cell sizes. The composites exhibited similar thermogravimetric weight change patterns under air. The weight loss below 373 K, which can be mostly attributed to the removal of physisorbed water, was 3−4%. The main weight loss event related to the combustion of carbon was centered at about 823 K and mainly took place in a narrow temperature interval (see Figure 3). The magnitude of this weight loss (taken from 673 K) was similar for all of the samples (29−33%). This weight loss is considered herein as approximate carbon content in the composites (see Table 1). The residue after the carbon had been burned out was 62−67% and can be regarded as an approximate SiO_2 content in the composites (see Table 1).

Nitrogen adsorption isotherms for the composites are shown in Figure 4. The composites exhibited relatively

(65) Kruk, M.; Jaroniec, M. *J. Phys. Chem. B* **2002**, *106*, 4732.
(66) Sing, K. S. W.; Everett, D. H.; Haul, R. A. W.; Moscou, L.; Pierotti, R. A.; Rouquerol, J.; Siemieniewska, T. *Pure Appl. Chem.* **1985**, *57*, 603.
(67) Kruk, M.; Jaroniec, M.; Gadkaree, K. P. *J. Colloid Interface Sci.* **1997**, *192*, 250.
(68) Kruk, M.; Jaroniec, M.; Sayari, A. *Langmuir* **1997**, *13*, 6267.

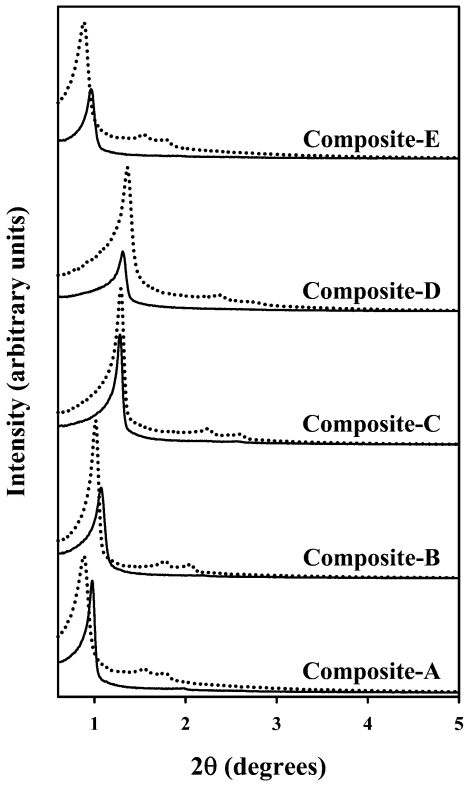

Figure 2. XRD patterns for the SBA-15 silica templates (dotted lines) and the corresponding SBA-15/carbon composites (solid lines).

Table 1. Structural Properties of SBA-15/Carbon Composites[a]

sample	a (nm)	S_{BET} (m^2 g^{-1})	V_t (cm^3 g^{-1})	$V_p + V_{mi}$ (cm^3 g^{-1})	S_{ex} (m^2 g^{-1})	w_{KJS} (nm)	% C	% SiO_2
composite A	10.5	410	0.32	0.29	10	5.2	29	67
composite B	9.4	370	0.27	0.25	10	4.9	29	67
composite C	8.0	470	0.32	0.31	<10	4.5	32	63
composite D	7.8	480	0.28	0.28	<10	3.7	30	64
composite E	10.6	360	0.27	0.24	10	4.9	33	62

[a] a, the unit-cell parameter for the 2-D hexagonal lattice; S_{BET}, the BET specific surface area; V_t, the total pore volume; $V_p + V_{mi}$, the sum of the primary mesopore volume and micropore volume; S_{ex}, the external surface area; w_{KJS}, the pore diameter calculated using the KJS method; % C, the carbon content (%) estimated as a thermogravimetric weight loss between 373 and 1023 or 1270 K under air; % SiO_2, aluminosilicate content (%) estimated as a residue at 1270 or 1023 K under air.

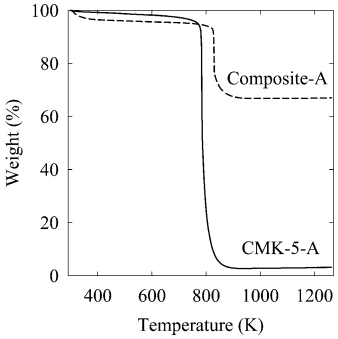

Figure 3. Weight change patterns for SBA-15/carbon composite A and the corresponding CMK-5-A carbon.

large adsorption at low pressures, which indicates the presence of micropores. There are several possible sources of microporosity in the composites. First, the carbonaceous film introduced on the surface of the OMS template is likely to be microporous to some extent. Second, there might be some accessible micropores between the carbon deposit and the template. Finally, some micropores originally present in the framework of the SBA-15 template[52,53] may also remain unfilled with carbon and accessible. The comparison of adsorption isotherms for the composites and for the CMK-5 carbons derived from them indicates that the last two of the above kinds of micropores provide a substantial contribution to the microporosity of the composites. Nitrogen adsorption isotherms for the composites exhibited more or less well-pronounced hysteresis loops that can be attributed to the capillary condensation−evaporation from the mesoporous interiors of the carbon pipes. The relative pressure at which the capillary condensation steps were observed and, consequently, the primary mesopore diameter[68] decreased for composites from A to D (for composite D, the step was poorly pronounced), as expected from the unit-cell size for these composites. In the case of composites A and E with the similar unit-cell size, the capillary condensation step was shifted to lower pressures for composite E, and thus the latter had a smaller pore diameter. Pore size distributions (Figure 5) allow one to better examine these trends in the pore diameter values, which ranged from 3.7 to 5.2 nm (see also Table 1). Clearly, the selection of SBA-15 templates with different unit-cell sizes allows one to obtain carbon nanopipes of different diameters. An additional control over the internal pipe diameter can be exercised through the variation of the amount of carbon introduced. In particular, composite E exhibited a slightly higher carbon/silica weight ratio than composite A, which allowed one to achieve a smaller primary mesopore diameter for the latter sample despite the similar unit-cell size for both of the composites. Apparently, the introduction of a larger relative amount of carbon resulted in the development of a thicker carbon film on the silica template surface, thus resulting in a larger reduction of diameter of the accessible pore space. The composites exhibited moderate BET specific surface areas (360−480 m^2 g^{-1}) and rather low total pore volumes (0.27−0.32 cm^3 g^{-1}). The micropore volume provided an appreciable contribution

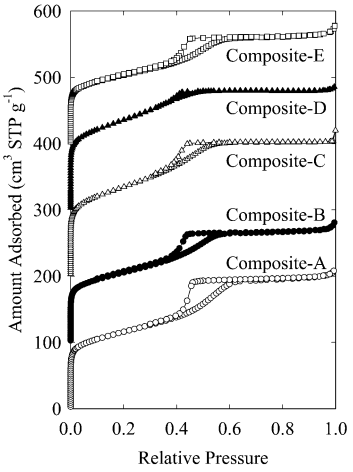

Figure 4. Nitrogen adsorption isotherms for the SBA-15/carbon composites. The isotherms for samples B, C, D, and E are offset vertically by 100, 200, 300, and 400 cm^3 STP g^{-1}, respectively.

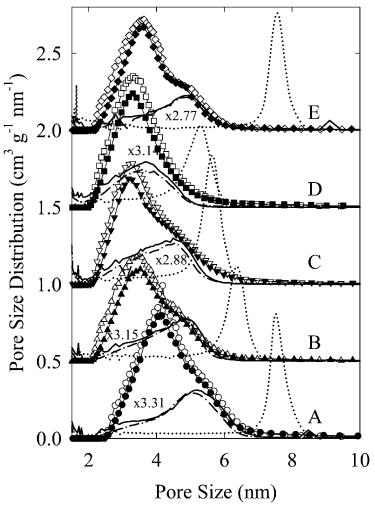

Figure 5. Pore size distributions (PSDs) calculated from nitrogen and argon adsorption isotherms for the SBA-15/carbon composites (thick lines) and the corresponding ordered mesoporous carbons (symbols and thin lines). The PSDs for pairs of samples B, C, D, and E were offset vertically by 0.5, 1, 1.5, and 2 cm^3 g^{-1} nm^{-1}, respectively. To facilitate the comparison between PSDs for the SBA-15/carbon composites and the corresponding carbons, the PSDs for the composites were multiplied by constants (see values on the figure) depending on the carbon contents in the composites and in the CMK-5 carbons. The PSDs for the SBA-15 samples obtained from the composites after the carbon deposit was burned out are denoted as dotted lines. The PSDs calculated for argon adsorption data are denoted as filled symbols and dash−dotted lines.

(at least 0.04−0.05 cm^3 g^{-1}, as evaluated using the α_s plot method) to the total pore volume.

From the point of view of the understanding of the CMK-5 structure, it is important to evaluate the thickness of walls of the carbon tubes. The latter thickness should be approximately equal to the thickness of the carbon film on the surface of the template in the SBA-15/carbon composites, because no appreciable changes in the rigid, 3-dimensionally connected carbon framework are expected as a result of the silica template dissolution. The thickness of the carbon film can be estimated as a difference between the radius of mesopores of the SBA-15 template in the composite and the radius of the mesopores of the composite. It is important to keep in mind that the pore diameter of the SBA-15 aluminosilicate used for the preparation of the composite is likely to decrease significantly during the carbonization step, which is carried out at a high temperature (1173 K). It is well-known that the SBA-15 pore size is significantly reduced when the calcination temperature is increased up to about 1273 K.[40,52] Therefore, the diameter of pores of the silica template in the composite was evaluated after the carbon was burned out from the composite through calcination under air at 873 K for 5 h. Because of the fact that this calcination temperature is much lower than the carbonization temperature (1173 K), no appreciable changes in the structure of the silica component of the composite are expected to result from the calcination. The isolated silica components of the composites were analyzed by using nitrogen adsorption (see Figure 6). These SBA-15 samples were found to exhibit appreciable adsorption capacity and narrow PSDs (see Figure 5).

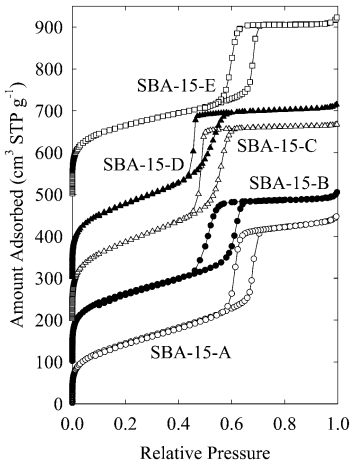

Figure 6. Nitrogen adsorption isotherms for SBA-15 samples obtained from the SBA-15/carbon composites by burning out carbon at 873 K for 5 h under air.

On the basis of the pore size analysis for the composites and for their silica components, the thickness of the carbon film was estimated to be in the range from 0.6 to 1.3 nm, depending on the particular composite. However, the broadness of PSDs for the SBA-15/carbon composites suggests some nonuniformity in the carbon film thickness, because the PSDs for the SBA-15 templates were appreciably narrower than those of the composites (see Figure 4). Further insight into the carbon film thickness uniformity was gained from the analysis of hysteresis loops on gas adsorption isotherms on the basis of the following considerations. Let us consider a pore that is wide enough to exhibit capillary condensation at pressure above the lower limit of adsorption−desorption hysteresis (that is, of diameter larger than ∼5 nm in the case of nitrogen adsorption or ∼4 nm in the case of argon adsorption at 77 K)[69,70] and is connected to the surrounding gas phase through a narrow entrance (or entrances). In this case, the capillary evaporation is delayed, either to the pressure at which the pore gains access to the surrounding gas phase through a continuous pathway of unfilled pore space or to the lower pressure limit of adsorption−desorption hysteresis, whichever of these two pressures is higher.[69−71] In other words, the capillary evaporation pressure from the pore that has access to the surrounding through narrower connecting pores takes place at the pressure of capillary evaporation from the connecting pore or, if the latter pressure is lower than the lower pressure limit of adsorption−desorption hysteresis, at the lower limit of hysteresis.[69,70] On the basis of this behavior, one can gain the following insight into the size of the connecting pores or constrictions in the porous structure. If the capillary evaporation from the pore takes place above the lower limit of hysteresis, the observed capillary evaporation pressure can be related to the pore entrance or constriction diameter. Under assumption of a particular shape of the pore entrance or constriction (for instance, cylindrical), the pore diameter−capillary evaporation relation can be estimated from studies of model pores of appropriate shape.[69,70] If the capillary evaporation takes place at the

(69) Kruk, M.; Jaroniec, M. *Chem. Mater.*, in press.
(70) Ravikovitch, P. I.; Neimark, A. V. *Langmuir* **2002**, *16*, 9830.
(71) Kruk, M.; Jaroniec, M. *Chem. Mater.* **2001**, *13*, 3169.

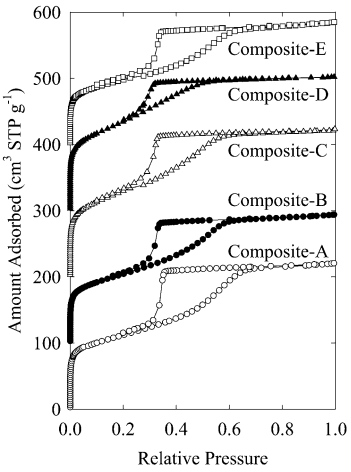

Figure 7. Argon adsorption isotherms at 77 K for the SBA-15/carbon composites. The isotherms for samples B, C, D, and E are offset vertically by 100, 200, 300, and 400 cm^3 STP g^{-1}, respectively.

lower limit of hysteresis, the size of the pore entrance or constriction can be estimated to be smaller than or equal to the size of the model pore that would exhibit capillary evaporation at the pressure that corresponds to the lower limit of hysteresis. At present, a cylindrical pore shape is the only one that is well understood from the point of view of its adsorption−desorption hysteresis behavior (see experimental[65,68] and theoretical[72] studies) and, at the same time, is appropriate as an approximation of the shape of the pore constriction or entrance.[69,70] However, this restriction does not appear to be a limiting factor in the analysis of the composites considered herein, which actually exhibit a cylindrical pore shape, and it is quite likely that constrictions in these pores (if any), would also be approximately circular in shape.

In the case of nitrogen adsorption at 77 K, the composites under study exhibited capillary condensation not far from the lower limit of adsorption−desorption hysteresis for nitrogen at 77 K, and capillary evaporation at the lower limit of hysteresis (relative pressure of 0.4−0.5[66,68]). Consequently, it was only possible to infer that the occurrence of constrictions in the mesopore structure of composites A, B, C, and E is quite likely, because the hysteresis loops on their nitrogen isotherms were not particularly narrow. To gain more insight, it was required to carry out gas adsorption under conditions at which the adsorption−desorption hysteresis extends to much lower pore diameters than in the case of nitrogen at 77 K. Argon at 77 K fulfills these requirements.[69,70] Argon adsorption isotherms for the composites are shown in Figure 7. It can be seen that these isotherms featured broad hysteresis loops with desorption branches that rapidly declined at the lower limit of adsorption−desorption hysteresis (the relative pressure somewhere between 0.27 and 0.38 for argon at 77 K, see results reported in refs 65, 69, and 70). Because of that, argon adsorption experiments also did not allow us to determine the exact size of the constrictions in the pipes. Nonetheless, hysteresis loops observed for the composites were clearly much broader than those observed for uniform cylindrical pores of similar size (widths below 0.06 relative pressure units were observed for highly ordered MCM-41 silicas with pore diameters from 3.5 to 4.8 nm),[65] thus strongly indicating that the interiors of the carbon pipes exhibited constrictions. The comparison of the relative pressure at which the hysteresis loops closed with the data for model cylindrical pores allowed us to draw a conclusion that the carbon pipes in the composites featured constrictions of diameter below about 3.5−3.8 nm. This suggests that the pipes have internal surfaces that are corrugated to an appreciable extent. This feature of the carbon pipes synthesized in the way employed herein has not been reported before. Now that the presence of corrugation or roughness on the internal surface of the carbon pipes is uncovered, it would be interesting to develop a methodology suitable for the introduction of a carbon film with a lower degree of corrugation or roughness. Argon adsorption at 77 K appears to be a useful technique to monitor the extent to which this goal is achieved in the case of the nanopipe synthesis. It is important to note that argon adsorption isotherms measured at 77 K not only provided information about the constrictions in the pore structures but also were suitable for the PSD assessment, which was highly consistent with that from nitrogen adsorption data (Figure 5).

3.3. CMK-5 Carbons. In the case of the inverse replication synthesis of CMK-3 carbon (which consists of arrays of 2-D hexagonally ordered carbon rods) through the complete filling of the SBA-15 template with the carbon precursor, the inverse carbon replica exhibited an XRD pattern similar to that of the SBA-15 template,[39,42] as well as to that for the corresponding SBA-15/carbon composite. A minor difference was that the XRD pattern for CMK-3 was somewhat less resolved and featured broader peaks than those observed on the XRD pattern for SBA-15. However, in the case of SBA-15/carbon composites in which carbon covers the surface of the template, but does not fill the entire pore space, the removal of the template to isolate the 2-D hexagonally ordered array of carbon tubes (CMK-5) led to significant changes in the XRD pattern, as reported earlier.[49] The main (100) peak dramatically decreased in intensity and became very weak, and consequently the (110) peak was the most intense peak on the XRD pattern for CMK-5. Similar changes in the XRD patterns were observed for the samples studied herein. As can be seen in Figure 8, the (100) peak was weak for the CMK-5 samples. On the other hand, a strong (110) reflection, usually accompanied by a (200) reflection, was observed for all of the carbons except for CMK-5-D, for which the (110) reflection was hardly discernible. The lower intensity of the (100) reflection in comparison to that for the (110) reflection was attributed to the diffraction interference between the pipe walls and the spacers interconnecting adjacent pipes.[49]

High-resolution TEM images of the CMK-5-A sample are shown in Figure 9. Figure 9a shows a hexagonally ordered array of circles and can be interpreted as a projection of the CMK-5 structure (Scheme 1) in the direction parallel to the pore channels. Figure 9b shows a pattern of uniformly spaced, parallel, dark stripes, each of which consists of a pair of parallel, dark lines. This image can be interpreted as a projection of the CMK-5 structure in the direction perpendicular to the pore channels. Wider, light stripes can be considered

(72) Neimark, A. V.; Ravikovitch, P. I. *Microporous Mesoporous Mater.* **2001**, *44*−*45*, 697.

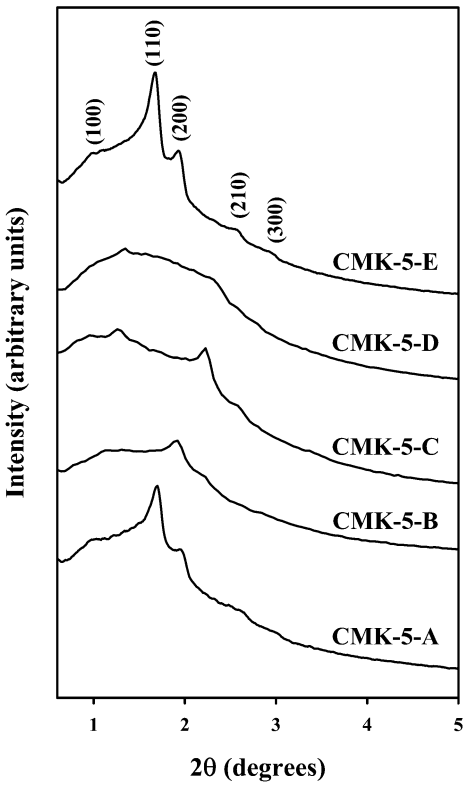

Figure 8. XRD patterns for the CMK-5 carbons.

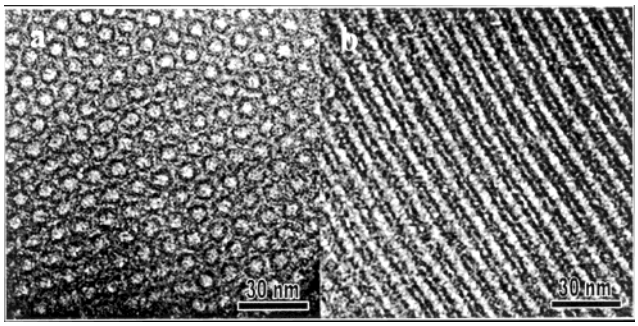

Figure 9. TEM images of CMK-5-A taken along the channel direction (a) and perpendicular to it (b).

as projections of the mesoporous interiors of the nanopipes, whereas the light lines between the pairs of closely spaced, dark lines can be considered as projections of the mesopores between the adjacent nanopipes.

The CMK-5 carbons appeared to be much more hydrophobic than the SBA-15/carbon composites, because the weight loss at temperatures below about 373 K, which can be attributed to the release of the physisorbed water, was very small (about 1%) despite the extremely high specific surface area of CMK-5. The combustion of the CMK-5 carbons under air was observed primarily in a narrow temperature range centered at about 780 K (see Figure 3). CMK-5 carbons proved to be more thermally stable under air than any of the CMK-1 carbons investigated in our previous study.[18] It should be noted that some OMCs were reported to exhibit thermal stability that was somewhat higher than that reported herein for CMK-5,[19,41] which in one of these cases may be related to the carbon precursor used.[19] The residue after the carbon combustion was about 3−6%, which indicated that the silica template dissolution was nearly complete.

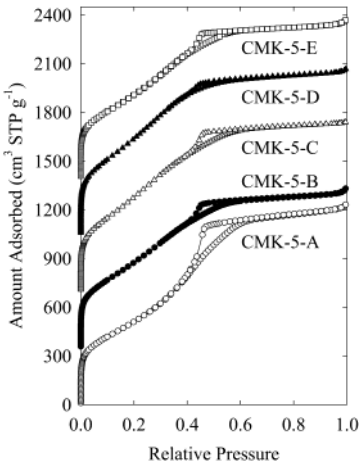

Figure 10. Nitrogen adsorption isotherms for the CMK-5 carbons. The isotherms for samples B, C, D, and E are offset vertically by 350, 700, 1050, and 1400 cm^3 STP g^{-1}, respectively.

Table 2. Structural Properties of CMK-5 Carbons[a]

sample	a (nm)	S_{BET} (m^2 g^{-1})	V_t (cm^3 g^{-1})	$V_p + V_{mi}$ (cm^3 g^{-1})	S_{ex} (m^2 g^{-1})	w_{KJS} (nm)
CMK-5-A	10.4	1850	1.89	1.72	100	4.2 (+shoulder)
CMK-5-B	9.2	1930	1.50	1.38	60	3.5 (+shoulder)
CMK-5-C	7.9	2120	1.60	1.53	50	3.3 (+shoulder)
CMK-5-D	7.7	2160	1.56	1.46	50	3.3
CMK-5-E	10.6	1860	1.48	1.38	50	3.6 (+shoulder)

[a] Notation: see Table 1.

Nitrogen adsorption isotherms for the CMK-5 samples are shown in Figure 10, and structural parameters derived from them, including the BET specific surface areas, total pore volumes, and pore diameters, are listed in Table 2. The CMK-5 carbons exhibited high adsorption capacity. The amount adsorbed increased up to the relative pressure of about 0.6−0.7, and subsequently the isotherms leveled off. Although the capillary condensation step was clearly distinct only for CMK-5-A, there was some evidence for the presence of capillary condensation steps on the isotherms for the other CMK-5 samples in the relative pressure range from about 0.2−0.3 to 0.5−0.6. The nitrogen adsorption isotherm reported earlier for a CMK-5 carbon sample featured two relatively well-separated capillary condensation steps related to the capillary condensation between the carbon pipes and in the interiors of the pipes.[49] In the case of the CMK-5 samples discussed herein, the capillary condensation steps related to adsorption in two different types of pores of CMK-5 were not separated (see Figure 10). Nonetheless, in all cases, there was some observable change in slope of the capillary condensation steps, which provided an indication that the step was a superposition of two overlapping steps. The existence of two different kinds of pores in the CMK-5 samples under study was more easily seen from the PSDs (Figure 5). The PSDs for all CMK-5 samples except for CMK-5-D featured a peak accompanied by a shoulder at somewhat higher pore size values. The shoulders were similar in position and shape to the PSDs for the corresponding SBA-15/carbon composites. Consequently, these shoulders reflect the pore size distribution of the internal pipe diameters, which overlaps with the size distribution of pores between the pipes. To allow for a better comparison between the PSDs for composites and

the carbons, the PSD values for the composites were multiplied by factors that would allow for the comparison of amounts adsorbed for the same weight of carbon in the samples of both types. So, the PSDs for the composites (after the proper multiplication, as indicated in Figure 5) can be considered as approximate contributions of the pipe interiors to the PSDs for the CMK-5 carbons. This identification allows one to conclude that the volume of pores between the pipes tends to be larger than the volume of the interiors of the pipes. This conclusion appears reasonable when one takes into account that, in the case of infinitely long pipes with smooth surface, the internal surface area is smaller than the external surface area, and the ratio between these two surface areas is equal to the ratio of the internal diameter to the external diameter of the pipe. Because of the fact that the diameters of the pores inside the pipes and the pores between the pipes appear to be quite similar, the larger extent of the external surface of the pipes (under the assumption of the surface smoothness) is likely to imply a larger volume of the pores between the pipes, consistent with the information from the PSDs (Figure 5).

The CMK-5 carbons exhibited the nitrogen BET specific surface areas between 1850 and 2160 m^2 g^{-1}. Even though these values may be somewhat overestimated[18] (for more reliable estimates based on argon data, see below), CMK-5 is certainly a material with a very high specific surface area, which tends to be larger than that of other OMCs reported to date. The remarkably high specific surface area of CMK-5 is likely to be related to its unique surface-templated structure. The total pore volume of CMK-5 samples under study was in the range from 1.48 to 1.72 cm^3 g^{-1}, which is also remarkably high, especially when one takes into account that this volume corresponds mostly to the volume of the ordered mesopores and the framework micropores, whereas the contribution from the volume of secondary mesopores is very small. Some other OMCs were reported to exhibit even higher total pore volumes,[33,47] but in one of these cases,[33] the secondary pore volume provided a significant contribution to the total pore volume, as inferred from the reported nitrogen adsorption isotherm. PSDs for CMK-5 carbons exhibited peaks centered at 3.3−4.2 nm (depending on the particular sample), which are related primarily to the presence of pores between the carbon pipes. However, the shoulders on the PSDs can be related to the size distribution of pores inside the pipes, as discussed above. The size of these pores can be tailored, as seen clearly from the above discussion of the properties of the SBA-15/carbon composites.

Argon adsorption isotherms measured at 77 K for the CMK-5 carbons are presented in Figure 11. Similarly to the argon isotherms for the composites, the isotherms for the CMK-5 carbons featured broad hysteresis loops, which indicates that adsorption properties of the pipe interiors were not modified to any appreciable extent during the silica template dissolution. The argon BET specific surface areas of the CMK-5 samples were very high (1550−1900 m^2 g^{-1}). PSDs evaluated for the carbons from argon adsorption data were found to be very similar to the PSDs determined from nitrogen adsorption data, which confirms our earlier findings that argon adsorption at 77 K is suitable for PSD calculations for pores of diameter below about 15 nm.[48,65]

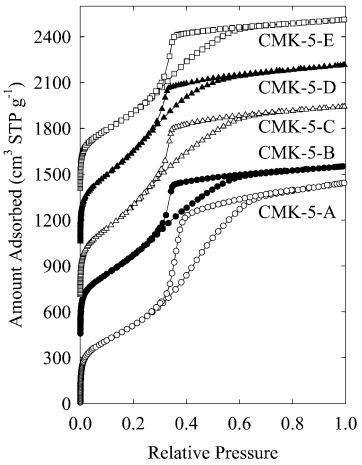

Figure 11. Argon adsorption isotherms for selected CMK-5 carbons. The isotherms for samples B, C, D, and E are offset vertically by 450, 700, 1050, and 1400 cm^3 STP g^{-1}, respectively.

4. Conclusions

We found out that the most important points in the CMK-5 synthesis using furfuryl alcohol were the incorporation of polymerization catalysts and the vacuum conditions during the pyrolysis. The proper selection of the SBA-15 template allows one to tailor both the external and internal diameter of carbon pipes in CMK-5. Moreover, the conditions for the introduction of the carbon precursor can be modified to achieve control of the internal pipe diameter without the modification of the external pipe diameter. CMK-5 carbons exhibit very high specific surface areas and pore volumes, which surpass those for many other ordered mesoporous carbons. This is likely to be related to the unique surface-templated rather than volume-templated structure of CMK-5. The SBA-15/carbon composites, which give rise to CMK-5 carbons after the SBA-15 template removal, have relatively low adsorption capacities. The thickness of walls of carbon pipes was estimated to be about 0.6−1.3 nm, depending on the particular sample. The argon adsorption study of these composites showed that the internal space in the carbon pipes features constrictions, and thus the pipes are likely to exhibit an appreciable surface roughness or corrugation. Studies in the direction of the introduction of more uniform carbon films on the silica surface are desirable.

Acknowledgment. The authors are grateful to Professor Osamu Terasaki at Stockholm University for providing TEM images. This work was supported in part by the donors of the Petroleum Research Fund administered by the American Chemical Society (M.J.), Creative Research Initiative Program of the Korean Ministry of Science and Technology (R.R.), and School of Molecular Science through the Brain Korea 21 project (R.R.).

CM034087+